

Grain size control of ZIF-8 MOF membranes by seeding-free aqueous synthesis and their performances in propylene/propane separation

Shunsuke Tanaka,^{a,b*} Kenta Okubo,^a Miki Sugita,^c Takahiko Takewaki^c

^aDepartment of Chemical, Energy and Environmental Engineering, Faculty of Environmental and Urban Engineering, Kansai University, 3-3-35 Yamate-cho, Suita-shi, Osaka 564-8680 JAPAN

^bOrganization for Research and Development of Innovative Science and Technology (ORDIST), Kansai University, 3-3-35 Yamate-cho, Suita-shi, Osaka 564-8680 JAPAN

^cYokohama Research Center, Mitsubishi Chemical Corporation, 1000 Kamoshida-cho, Aoba-ku, Yokohama 227-8502 JAPAN

* Corresponding author

Tel/Fax: +81-6-6368-0851; E-mail: shun_tnk@kansai-u.ac.jp (S. Tanaka)

ABSTRACT

Polycrystalline ZIF-8 membranes of about 1 μm in thickness were successfully grown on α -alumina porous support by seeding-free aqueous synthesis. In order to achieve continuous well-intergrown membranes, a pseudo-surface of ZIF-8 was formed on the support by chemical modification. Our membrane preparation in aqueous system is based on the support-surface activation concept to control the surface density of nucleation sites. The grain size of polycrystalline membrane is directly related to a graft density of ligand-analogous surface modifier. Single-component gas permeation properties were investigated using H_2 , CO_2 , N_2 , CH_4 , C_3H_6 , and C_3H_8 . While the ideal permselectivities of H_2 from CO_2 , N_2 , CH_4 , and C_3H_6 ever so slightly increased with the graft density, the ideal permselectivity of $\text{C}_3\text{H}_6/\text{C}_3\text{H}_8$ increased rapidly and reached 36 with corresponding C_3H_6 permeance of $8.5 \times 10^{-8} \text{ mol/m}^2 \cdot \text{s} \cdot \text{Pa}$. As a conclusion of the combined characterization with adsorption analysis, it was found that the sieving of $\text{C}_3\text{H}_6/\text{C}_3\text{H}_8$ by our seeding-free aqueous-synthesized ZIF-8 membrane is mainly governed by diffusion-driven separation process.

KEYWORDS

ZIF-8, Structural flexibility, In situ growth, Grain size, $\text{C}_3\text{H}_6/\text{C}_3\text{H}_8$ separation

1. INTRODUCTION

Metal organic frameworks (MOFs)[1–4] offer many interesting opportunities in separation/reaction technology, with unprecedented capacities and chemical and structural tunability. Zeolitic imidazolate frameworks (ZIFs) are a subfamily of MOFs. They share the same topology with zeolites but consist of metal nodes (usually Zn or Co) bridged by imidazole-based linkers to form neutral open framework structures.[5–7] ZIFs have been recognized as unique molecular sieving materials with flexible framework, enabling the possibility of simultaneous high permeability and attractive selectivity for use in membrane-based separations.[8–10] Among the many ZIFs, ZIF-8 ($\text{Zn}(\text{2-methylimidazole})_2$) is undoubtedly the most extensively studied due to its facile synthesis coupled with its exceptional chemical and thermal stabilities.[11] ZIF-8 crystallizes into the sodalite topology, forming the large cages (diameter of 11.6 Å) interconnected via narrow 6-ring windows (3.4 Å). Such framework structure gives ZIF-8 particularly interesting “gate-opening” functionality. Numerous experimental and computational studies have revealed that the pore apertures swing open by reorientation of imidazolate linkers and expand when probed with guest molecules.[12–18] It is suggested that the effective aperture size of ZIF-8 is 4.0–4.2 Å. ZIF-8 is an ideal candidate for membrane-based propylene/propane separation rather than for hydrogen purification and CO_2 separation. In addition, our previous results revealed that “gate-opening” functionality and transport property of ZIF-8 are strongly affected by crystal size,[19] suggesting high potential for control of membrane separation performance with crystal size.

So far, several research groups have reported diverse synthesis protocols for ZIF-8 membranes. Most of the protocols are generally derived from those devised for zeolite membrane preparation.[20–27] In order to achieve well-intergrown polycrystalline ZIF-8 membranes, it is essential to control

heterogeneous nucleation and membrane growth on porous support with avoiding homogeneous nucleation and crystal growth in bulk solution. To promote the heterogeneous nucleation and membrane growth, in situ growth techniques have been developed to improve ZIF deposition by chemical modification of support surface.[28–32] In our previous work, we first applied the chemical modification of support surface for ZIF-8 membrane preparation in an aqueous system.[33,34] Such support-surface activation approaches also undertake a role to anchor the coordinating ZIF crystals on support.

Here we report a grain size control of polycrystalline ZIF-8 membranes by chemical modification of support surface. Our membrane preparation in aqueous system is based on the support-surface activation concept to control the surface density of nucleation sites. Aqueous synthesis at room temperature is more economical and greener compared to other synthesis procedures in organic solvents.[35] In order to provide the active sites for nucleation, a pseudo-surface of ZIF-8 was formed on the support surface by 3-(2-imidazolin-1-yl)propyltriethoxysilane (IPTES) modification. The IPTES is surface modification agent with imidazoline end group, which is analogous to the imidazolate linker of ZIF-8 and then coordinates with Zn and acts as nucleation site. Our strategy is based on the expectation that the grain size of polycrystalline membrane is directly related to the nucleation density on support-surface and can generally determined by number of grains. In this work, we prepared well-intergrown polycrystalline ZIF-8 membranes with difference in grain size by controlling the graft density of IPTES on porous α -alumina support and studied gas permeation with focus on C_3H_6/C_3H_8 separation.

2. EXPERIMENT

2.1 IPTES modification of the support surface

Porous α -alumina tubular supports (outer diameter: 10 mm; inner diameter: 7 mm; length: 20 mm; average porosity: 35%; average pore size: 0.15 μm) were used as a support. One side of the tubular supports was connected to a dense glass plate with epoxy-based sealant prior to surface modification. The supports with dead-end structure were treated with IPTES (0–30 g/L in 10 mL of 0.01 M HCl) at 90 °C for 10 min with the aid of microwave irradiation, followed by washing with deionized water. The graft density of IPTES on porous α -alumina support was estimated from the remaining IPTES in the solution. The remaining concentration of Si in the solution was measured using an inductively coupled plasma (ICP) emission spectroscopy (ICPS-7510, Shimadzu). The graft density was calculated by the following equation:

$$\rho = \frac{N_{\text{Si}}}{S_{\text{BET}}m_{\text{support}}}$$

where N_{Si} is the substance quantity of IPTES consumed in the surface modification, S_{BET} is the specific surface area of the support (2.1 m^2/g), and m_{support} is the mass of the dried support.

2.2 Membrane preparation and characterization

ZIF-8 membranes were grown on the IPTES-grafted supports as follows: The supports were vertically immersed in a precursor solution consisting of deionized water, zinc acetate, and 2-methylimidazole (Hmim) at room temperature. The molar composition of the solution was Zn : Hmim : water = 1 : 30 : 2228. The obtained membranes were washed with 0.1 M Hmim methanol solution and then dried at room temperature. Finally, the membranes were dried at 50 °C under vacuum.

X-ray diffraction (XRD) patterns were recorded on a RINT-TTR III X-ray diffractometer (Rigaku, Japan) using $\text{CuK}\alpha$ radiation at 40 kV and 20 mA. Field emission scanning electron microscopy (FESEM) images of membrane were obtained using an S-4800 electron microscope (Hitachi High-Tech, Japan) operated at an acceleration voltage of 1–10 kV.

2.3 Evaluation of gas permeation

Single gas permeation measurements were carried out for gases, H_2 , CO_2 , N_2 , CH_4 , C_3H_6 , C_3H_8 , at 25 °C. The α -alumina-supported ZIF-8 membranes were activated at 50 °C under vacuum for 6 h prior to the measurements and then sealed with silicon O-ring in a stainless steel permeation cell. The driving force across the membrane was provided by pressure drop. In all permeation measurements, the pressure drop was kept constant at 0.1 MPa and the permeation side was kept constant at atmospheric pressure. The permeate flow rate was measured with a soap film bubble flow meter. The permeances were calculated as the fluxes divided by the driving force. The ideal separation selectivity was determined as the ratio of the permeances of the pure compounds.

Binary component gas permeation measurements were carried out for an equimolar $\text{C}_3\text{H}_6/\text{C}_3\text{H}_8$ mixture at 25 °C. The mixture was supplied to a feed side while a permeate side was swept by He with the total flow rates of both sides maintained at 100 ml/min. The compositions of the steady state feed, retentate, and permeate were analyzed using gas chromatography (GC-2014, Shimadzu).

3. RESULTS AND DISCUSSION

3.1 Membrane growth

Figure 1 shows the variation of the graft density of IPTES on porous α -alumina support as a function of IPTES concentration. The graft density increases while increasing the IPTES concentration until a plateau value at around $1.8 \mu\text{mol}/\text{m}^2$. The adequacy of the surface modification amount was double-checked by measurement of variation in the weight of base material. With the α -alumina-support, however, since there is significantly low surface area of the support, quantitative experimental investigation was very difficult. Thus, silica powder with relatively high surface area ($310 \text{ m}^2/\text{g}$) was used for gravimetric measurement. When the IPTES concentration was 30 g/L , the graft density of IPTES on silica powder was estimated to be $2.6 \mu\text{mol}/\text{m}^2$ by ICP elemental analysis. After the surface modification, silica powder increased in weight by 13%. The weight loss in the temperature range $250\text{--}500 \text{ }^\circ\text{C}$, which is mainly attributed to the decomposition of 3-(2-imidazolin-1-yl)propyl group, was 8%, corresponding to $2.3 \mu\text{mol}/\text{m}^2$, which is good agreement with the evaluation by ICP elemental analysis. The single gas permeance of N_2 at $25 \text{ }^\circ\text{C}$ through the highest-grafted α -alumina-support was $9.2 \times 10^{-7} \text{ mol}/\text{m}^2 \cdot \text{s} \cdot \text{Pa}$, which is not much different from the bare support ($9.3 \times 10^{-7} \text{ mol}/\text{m}^2 \cdot \text{s} \cdot \text{Pa}$); in other words, the permselectivity characteristics are independent of graft density of IPTES on porous α -alumina support.

The morphologies of the α -alumina-supported ZIF-8 membranes were investigated by FESEM. The images of ZIF-8 membranes grown on the IPTES-grafted support with different graft densities are shown in **Figure 2**. The grains of resulting ZIF-8 membranes were well-intergrown on the IPTES-grafted supports. On the other hand, such well-intergrown crystals and well-defined facets were not formed on the unmodified support. Even though the reflection peaks ascribed to ZIF-8 appeared for product formed on the unmodified support as shown in **Figure 3**, top-view of support showed that the

external surface still retained remnant of the original alumina grain structure. These results suggest that the ZIF-8 layer was thinly-deposited on the unmodified alumina surface.

Of particular interest is grain downsizing of polycrystalline ZIF-8 membrane with increasing graft density of IPTES (**Figure 2**). The number of ZIF-8 grains on the support with an area of more than $100 \mu\text{m}^2$ was measured to discuss the grain size. **Figure 4** shows the number density of ZIF-8 grains on the IPTES-grafted support. The number density of ZIF-8 grains increased with increasing graft density of IPTES, which also supports the grain downsizing of polycrystalline ZIF-8 membrane. Although further investigation is needed to understand the grain structure in the direction perpendicular to the membrane surface, these results indicate that ZIF-8 preferentially nucleated and grew on the IPTES-grafted surface. ZIF-8 formation occurs via a coordination reaction between the zinc ions and deprotonated Hmim (mim^-). The mim^- ligand is highly symmetric and exists in two equivalent tautomeric forms, because the proton can be located on either of the two nitrogen atoms. Under appropriately basic conditions, a nitrogen atom of mim^- coordinates to a Zn atom of the adjacent unit to construct the crystal assembly.[35] **Figure 5** illustrates the heterogeneous nucleation and membrane growth of polycrystalline ZIF-8 membranes on the IPTES-grafted surface. In order to provide active sites for nucleation, a pseudo-surface of ZIF-8 is formed on the pore surface of α -alumina support using IPTES. The imidazoline end group of IPTES is analogous to the mim^- ligand and then coordinates with Zn and induces the heterogeneous nucleation on the support-surface. In this membrane preparation, the grain size of polycrystalline ZIF-8 membrane is determined by the nucleation density on support-surface and can be controlled by the graft density of surface modifier. On the other hand, there is no large difference in the membrane thickness. The membranes were all similar about $1 \mu\text{m}$ thick.

The reflection peak intensities were all similar for ZIF-8 membranes consisted of different grain sizes, indicating no large difference in ZIF-8 crystallinity. Although the low intensity may be attributed to (1) the low sample weight due to thin membrane morphology, (2) the composite structure with support, and/or (3) the unavoidable displacement of specimen in the XRD measurement due to the geometry of the curved support, the resulting ZIF-8 crystals were unlikely to make much of a structural and chemical difference. This result allows a proper assessment of the effect of grain downsizing on gas permeation properties of polycrystalline ZIF-8 membrane.

3.2 Gas permeation properties

The single-component gas permeation properties were investigated at 25 °C using H₂, CO₂, N₂, CH₄, C₃H₆, C₃H₈, with increasing molecular diameters. The scale of kinetic diameters was adopted for this study as the molecular size.[36] As shown in **Figure 6**, the permeance decreased rapidly with increasing molecular size of the permeating gas. H₂ shows the highest permeance among the gases investigated, C₃H₆ and C₃H₈ can still permeate even though they are larger than the crystallographic size of six-ring window of ZIF-8.

At the graft density of IPTES of 1.9 μmol/m², the H₂ permeance was 2.3 × 10⁻⁷ mol/m²·s·Pa and the ideal permselectivities of H₂/CO₂, H₂/N₂, H₂/CH₄, H₂/C₃H₆, and H₂/C₃H₈ were 6.2, 13.7, 14.8, 26.5, and 953, respectively, which considerably exceeds the Knudsen diffusion selectivities. These results indicate that the ZIF-8 membranes prepared by our seeding-free aqueous synthesis possess a good molecular-sieving property. The ideal permselectivities of H₂ from CO₂, N₂, CH₄, and C₃H₆ ever so slightly increased with the graft density of IPTES. On the other hand, the ideal permselectivity of C₃H₆/C₃H₈ increased rapidly with the graft density of IPTES (**Figure 7**). The performance of

polycrystalline membranes strongly depends on the membrane microstructure. As discussed in our previous reports, aqueous synthesis occurs extremely-fast formation of ZIF-8 crystals.[34,35] The difference in permselectivities for C_3H_6/C_3H_8 may be due to a slight difference in microstructures coupled with grain size.

3.3 Propylene/propane separation

Recent studies have focused on the performance of ZIF-8 for C_3H_6/C_3H_8 separation.[11] It is one of the most difficult yet critical processes for the petroleum and chemical industry. For our ZIF-8 membranes, the ideal permselectivity increased with increasing graft density of IPTES (**Figure 7**). The C_3H_6/C_3H_8 permeance slightly decreased and selectivity increased with increasing graft density of IPTES, in other words, with the grain downsizing.

It is interesting to note that ZIF-8 membranes can pass and sieve C_3H_6 and C_3H_8 even though their kinetic diameters are larger than the crystallographic size of six-ring window of ZIF-8. These permeation behaviors are attributed to the framework flexibility. It is well known that ZIF-8 can adsorb molecules as large as 7.6 Å (1,2,4-trimethylbenzene).[37] This unexpected adsorption behavior has been speculated to be due to the flexible apertures that swing open by reorientation of imidazolate linkers enforced by guest adsorption.[15–18] In the first place, adsorption isotherms of C_3H_6 and C_3H_8 on the aqueous-synthesized ZIF-8 powder sample were measured. The adsorption isotherms were measured at different temperature to determine the isosteric heat of adsorption. As shown in **Figure 8**, there is no large difference in static adsorption property of ZIF-8, adsorbed amount and adsorption heat, between C_3H_6 and C_3H_8 . ZIF-8 can adsorb C_3H_6 and C_3H_8 , corresponding to the accommodation of 6 molecules per cage. On the other hand, there is difference in adsorption kinetics of C_3H_6 and C_3H_8 , as

shown in **Figure 9** and **Table 1**. C_3H_6 has higher diffusivities with smaller activation energy for diffusion compared with C_3H_8 . On the ZIF-8 powder prepared in aqueous system, the C_3H_6 diffusivities are about 10 to 30 times higher than those of C_3H_8 . The permeance ratio of C_3H_6/C_3H_8 for our ZIF-8 membranes reaches 36. These results indicate that the sieving of C_3H_6/C_3H_8 by our seeding-free aqueous-synthesized ZIF-8 membrane is mainly governed by diffusion-driven separation process. At the graft density of IPTES of 1.7 and 1.9 $\mu\text{mol}/\text{m}^2$, the permselectivities for an equimolar C_3H_6/C_3H_8 mixture were 11.3 and 31.3, respectively. C_3H_6/C_3H_8 permselectivity was slightly lower in the binary mixture as compared to ideal permselectivity, due to cooperative diffusion effect, which enhances C_3H_8 diffusion in the presence of C_3H_6 .

Finally, the fact that the support surface chemistry can affect both heterogeneous nucleation and crystallization was well applied for polycrystalline ZIF-8 membrane preparation. Our results established a correlation between the graft density of surface modifier and the grain structure. The grain downsizing should result in an increase in the interfaces that can be potential cause of membrane defects. The membrane densification is necessary since membranes without intergrain pores are required to utilize only the inherent pores of the ZIF-8 structure. However, the fact that the membranes with smaller grain size exhibit higher permselectivity may be due to that the crystallization is dominated by the presence of heterogeneous nucleation sites, and thus the increase in the graft density is accompanied by high crystallization and improving densification processes of the polycrystalline ZIF-8 membrane.

On the other hand, ZIF-8 has been recognized as a unique molecular sieving material with flexible framework, enabling interesting “gate-opening” functionality. More recently, it is recognized that controlling the crystal size and shape is an effective factor for regulating the structural flexibilities and

mass transport properties.[19,38] The change in the structural flexibilities and mass transport properties due to the grain downsizing may also partially contribute to improvement of permselective performance. An interesting approach is to utilize the crystal size dependency of structural transitions and adsorption dynamics of ZIF-8 during guest molecule diffusion. Consequently, grain size engineering of polycrystalline ZIF-8 membranes potentially improves the membrane permselective performance. To take advantage of this unique adsorption property for membrane separation, further systematic control in the structural flexibilities is of crucial importance.

4. CONCLUSIONS

In this study, high-quality ZIF-8 membranes were successfully grown on the IPTES-modified porous supports by aqueous synthesis. In this membrane preparation, the imidazoline end group of IPTES is analogous to the mim^- ligand and then coordinates with Zn and induces the nuclei formation of ZIF-8. The advantage of this method is that the graft density of IPTES can control the grain size of polycrystalline ZIF-8 membrane. The ZIF-8 membranes showed a good molecular-sieving property. The ideal permselectivity of $\text{C}_3\text{H}_6/\text{C}_3\text{H}_8$ increased with the graft density of IPTES and reached 36 with corresponding C_3H_6 permeance of $8.5 \times 10^{-8} \text{ mol/m}^2 \cdot \text{s} \cdot \text{Pa}$. Aqueous synthesis combined with the support-surface activation concept is more economical and greener compared to other synthesis procedures in organic solvents. Further studies are under way to control the grain size of polycrystalline MOF membranes over a wide range from nanometer to micrometer size for improvement of the membrane permselective performance.

ACKNOWLEDGEMENTS

This work was financially supported by the Kansai University fund for Supporting Young Scholars, 2015. S. Tanaka acknowledges Yashima Environment Technology Foundation.

Table 1 Calculated diffusivity^a of C₃H₆ and C₃H₈ into the aqueous synthesized ZIF-8

Temperature (°C)	$D_{\text{C}_3\text{H}_6}$ (m ² /s)	$D_{\text{C}_3\text{H}_8}$ (m ² /s)
15	5.48×10^{-13}	2.33×10^{-14}
25	5.70×10^{-13}	2.63×10^{-14}
35	5.84×10^{-13}	3.75×10^{-14}
45	5.88×10^{-13}	4.26×10^{-14}

^a Diffusivity calculated by simply fitting an intracrystalline (Fick) diffusion model.

Figure captions

Figure 1 Variation of the graft density of IPTES on porous α -alumina support as a function of IPTES concentration.

Figure 2 Top-view and cross-sectional FESEM images of ZIF-8 membranes prepared on porous support with different graft densities of IPTES (scale bar: 2 μm).

Figure 3 XRD patterns of ZIF-8 membranes prepared on porous support with different graft densities of IPTES.

Figure 4 Variation of the number density of ZIF-8 grains on porous α -alumina support as a function of the graft density of IPTES.

Figure 5 Schematic illustration of the heterogeneous nucleation and crystal growth on the IPTES-grafted surface. The ligand-analogous surface modifier induces preferential heterogeneous nucleation and determines the grain size of polycrystalline ZIF-8 membrane.

Figure 6 Single-component gas permeations in relation to the kinetic diameters of the gases. ZIF-8 membranes were prepared on porous support with different graft densities of IPTES.

Figure 7 Changes in C_3H_6 permeance and $\text{C}_3\text{H}_6/\text{C}_3\text{H}_8$ permselectivities with graft density of IPTES.

Figure 8 Adsorption isotherms (top) and isosteric adsorption heat (bottom) of C_3H_6 and C_3H_8 in ZIF-8.

Figure 9 Uptake curves of C_3H_6 and C_3H_8 in ZIF-8. Arrhenius plot of diffusivities for C_3H_6 and C_3H_8 (inset).

References

- [1] M. Kondo, T. Yoshitomi, H. Matsuzaka, S. Kitagawa, K. Seki, Three-dimensional framework with channeling cavities for small molecules: $\{[M_2(4,4'\text{-bpy})_3(\text{NO}_3)_4] \cdot x\text{H}_2\text{O}\}_n$ ($M = \text{Co}, \text{Ni}, \text{Zn}$), *Angew. Chem., Int. Ed.* 36 (1997) 1725–1727.
- [2] H. Li, M. Eddaoudi, M. O’Keeffe, O. M. Yaghi, Design and synthesis of an exceptionally stable and highly porous metal-organic framework, *Nature* 402 (1999) 276–279.
- [3] O. M. Yaghi, M. O’Keeffe, N. W. Ockwig, H. K. Chae, M. Eddaoudi, J. Kim, Reticular synthesis and the design of new materials, *Nature* 423 (2003) 705–714.
- [4] G. Férey, Hybrid porous solids: Past, present, future, *Chem. Soc. Rev.* 37 (2008) 191–214.
- [5] K. S. Park, Z. Ni, A. P. Cote, J. Y. Choi, R. D. Huang, F. J. Uribe-Romo, H. K. Chae, M. O’Keeffe, O. M. Yaghi, Exceptional chemical and thermal stability of zeolitic imidazolate frameworks, *Proc. Natl. Acad. Sci. U. S. A.* 103 (2006) 10186–10191.
- [6] R. Banerjee, A. Phan, B. Wang, C. Knobler, H. Furukawa, M. O’Keeffe, O. M. Yaghi, High-throughput synthesis of zeolitic imidazolate frameworks and application to CO_2 capture, *Science* 319 (2008) 939–943.
- [7] A. Phan, C. J. Doonan, F. J. Uribe-Romo, C. B. Knobler, M. O’Keeffe, O. M. Yaghi, Synthesis, structure, and carbon dioxide capture properties of zeolitic imidazolate frameworks, *Acc. Chem. Res.* 43 (2010) 58–67.

- [8] J. R. Li, R. J. Kuppler, H. C. Zhou, Selective gas adsorption and separation in metal-organic frameworks, *Chem. Soc. Rev.* 38 (2009) 1477–1504.
- [9] M. Shah, M. C. McCarthy, S. Sachdeva, A. K. Lee, H. K. Jeong, Current status of metal-organic framework membranes for gas separations: promises and challenges, *Ind. Eng. Chem. Res.* 51 (2012) 2179–2199.
- [10] J. Yao, H. Wang, Zeolitic imidazolate framework composite membranes and thin films: Synthesis and applications, *Chem. Soc. Rev.* 43 (2014) 4470–4493.
- [11] C. Zhang, W. J. Koros, Zeolitic imidazolate framework-enabled membranes: Challenges and opportunities, *J. Phys. Chem. Lett.* 6 (2015) 3841–3849.
- [12] J. Pérez-Pellitero, H. Amrouche, F. R. Siperstein, G. Pirngruber, C. Nieto-Draghi, G. Chaplais, A. Simon-Masseron, D. Bazer-Bachi, D. Peralta, N. Bats, Adsorption of CO₂, CH₄, and N₂ on zeolitic imidazolate frameworks: Experiments and simulations, *Chem. –Eur. J.* 16 (2010) 1560–1571.
- [13] M. T. Luebbers, T. J. Wu, L. J. Shen, R. I. Masel, Effects of molecular sieving and electrostatic enhancement in the adsorption of organic compounds on the zeolitic imidazolate framework ZIF-8, *Langmuir* 26 (2010) 15625–15633.
- [14] D. Fairen-Jimenez, S. A. Moggach, M. T. Wharmby, P. A. Wright, S. Parsons, T. Düren, Opening the gate: Framework flexibility in ZIF-8 explored by experiments and simulations, *J. Am. Chem. Soc.* 133 (2011) 8900–8902.

- [15] S. A. Moggach, T. D. Bennett, A. K. Cheetham, The effect of pressure on ZIF-8: Increasing pore size with pressure and the formation of a high-pressure phase at 1.47 GPa, *Angew. Chem., Int. Ed.* 48 (2009) 7087–7089.
- [16] C. O. Ania, E. García-Pérez, M. Haro, J. J. Gutiérrez-Sevillano, T. Valdés-Solís, J. B. Parra, S. Calero, Understanding gas-induced structural deformation of ZIF-8, *J. Phys. Chem. Lett.* 3 (2012) 1159–1164.
- [17] L. Zhang, Z. Hu, J. Jiang, Sorption-induced structural transition of zeolitic imidazolate framework-8: A hybrid molecular simulation study, *J. Am. Chem. Soc.* 135 (2013) 3722–3728.
- [18] H. Tanaka, S. Ohsaki, S. Hiraide, D. Yamamoto, S. Watanabe, M. T. Miyahara, Adsorption-induced structural transition of ZIF-8: A combined experimental and simulation study, *J. Phys. Chem. C* 118 (2014) 8445–8454.
- [19] S. Tanaka, K. Fujita, Y. Miyake, M. Miyamoto, Y. Hasegawa, T. Makino, S. Van der Perre, J. C. S. Remi, T. Van Assche, G. V. Baron, J. F. M. Denayer, Adsorption and diffusion phenomena in crystal size engineered ZIF-8 MOF, *J. Phys. Chem. C* 119 (2015) 28430–28439.
- [20] S. R. Venna, M. A. Carreon, Highly permeable zeolite imidazolate framework-8 membranes for CO₂/CH₄ separation, *J. Am. Chem. Soc.* 132 (2010) 76–78.
- [21] H. Bux, A. Feldhoff, J. Cravillon, M. Wiebcke, Y. S. Li, J. Caro, Oriented zeolitic imidazolate framework-8 membrane with sharp H₂/C₃H₈ molecular sieve separation, *Chem. Mater.* 23 (2011) 2262–2269.

- [22]K. Tao, C. L. Kong, L. Chen, High performance ZIF-8 molecular sieve membrane on hollow ceramic fiber via crystallizing-rubbing seed deposition, *Chem. Eng. J.* 220 (2013) 1–5.
- [23]Y. C. Pan, Z. P. Lai, Sharp separation of C₂/C₃ hydrocarbon mixtures by zeolitic imidazolate framework-8 (ZIF-8) membranes synthesized in aqueous solutions, *Chem. Commun.* 47 (2011) 10275–10277.
- [24]Y. C. Pan, T. Li, G. Lestari, Z. P. Lai, Effective separation of propylene/propane binary mixtures by ZIF-8 membranes, *J. Membr. Sci.* 390–391 (2012) 93–98.
- [25]Y. C. Pan, B. Wang, Z. P. Lai, Synthesis of ceramic hollow fiber supported zeolitic imidazolate framework-8 (ZIF-8) membranes with high hydrogen permeability, *J. Membr. Sci.* 421–422 (2012) 292–298.
- [26]J. F. Yao, L. X. Li, W. H. B. Wong, C. Z. Tan, D. H. Dong, H. T. Wang, Formation of ZIF-8 membranes and crystals in a diluted aqueous solution, *Mater. Chem. Phys.* 139 (2013) 1003–1008.
- [27]D. F. Liu, X. L. Ma, H. X. Xi, Y. S. Lin, Gas transport properties and propylene/propane separation characteristics of ZIF-8 membranes, *J. Membr. Sci.* 451 (2014) 85–93.
- [28]A. S. Huang, H. Bux, F. Steinbach, J. Caro, Molecular-sieve membrane with hydrogen permselectivity: ZIF-22 in LTA topology prepared with 3-aminopropyltriethoxysilane as covalent linker, *Angew. Chem. Int. Ed.* 49 (2010) 4958–4961.

- [29] A. S. Huang, W. Dou, J. Caro, Steam-stable zeolitic imidazolate framework ZIF-90 membrane with hydrogen selectivity through covalent functionalization, *J. Am. Chem. Soc.* 132 (2010) 15562–15564.
- [30] A. S. Huang, J. Caro, Covalent post-functionalization of zeolitic imidazolate framework ZIF-90 membrane for enhanced hydrogen selectivity, *Angew. Chem. Int. Ed.* 50 (2011) 4979–4982.
- [31] A. S. Huang, Y. F. Chen, N. Y. Wang, Z. Q. Hu, J. W. Jiang, J. Caro, A highly permeable and selective zeolitic imidazolate framework ZIF-95 membrane for H₂/CO₂ separation, *Chem. Commun.* 48 (2012) 10981–10983.
- [32] K. Huang, Z. Y. Dong, Q. Q. Li, W. Q. Jin, Growth of a ZIF-8 membrane on the inner-surface of a ceramic hollow fiber *via* cycling precursors, *Chem. Commun.* 49 (2013) 10326–10328.
- [33] K. Kida, K. Fujita, T. Shimada, S. Tanaka, Y. Miyake, Layer-by-layer aqueous rapid synthesis of ZIF-8 films on a reactive surface, *Dalton Trans.* 42 (2013) 11128–11135.
- [34] S. Tanaka, T. Shimada, K. Fujita, Y. Miyake, K. Kida, K. Yogo, J. F. M. Denayer, M. Sugita, T. Takewaki, Seeding-free aqueous synthesis of zeolitic imidazolate framework-8 membranes: How to trigger preferential heterogeneous nucleation and membrane growth in aqueous rapid reaction solution, *J. Membr. Sci.* 472 (2014) 29–38.
- [35] K. Kida, M. Okita, K. Fujita, S. Tanaka, Y. Miyake, Formation of high crystalline ZIF-8 in an aqueous solution, *CrystEngComm* 15 (2013) 1794–1801.

- [36]C. Zhang, R. P. Lively, K. Zhang, J. R. Johnson, O. Karvan, W. J. Koros, Unexpected molecular sieving properties of zeolitic imidazolate framework-8, *J. Phys. Chem. Lett.* 3 (2012) 2130–2134.
- [37]K. Zhang, R. P. Lively, C. Zhang, R. R. Chance, W. J. Koros, D. S. Sholl, S. Nair, Exploring the framework hydrophobicity and flexibility of ZIF-8: From biofuel recovery to hydrocarbon separations, *J. Phys. Chem. Lett.* 4 (2013) 3618–3622.
- [38]S. Watanabe, S. Ohsaki, T. Hanafusa, K. Takada, H. Tanaka, K. Mae, M. T. Miyahara, Synthesis of zeolitic imidazolate framework-8 particles of controlled sizes, shapes, and gate adsorption characteristics using a central collision-type microreactor, *Chem. Eng. J.* 313 (2017) 724–733.

Figure 1

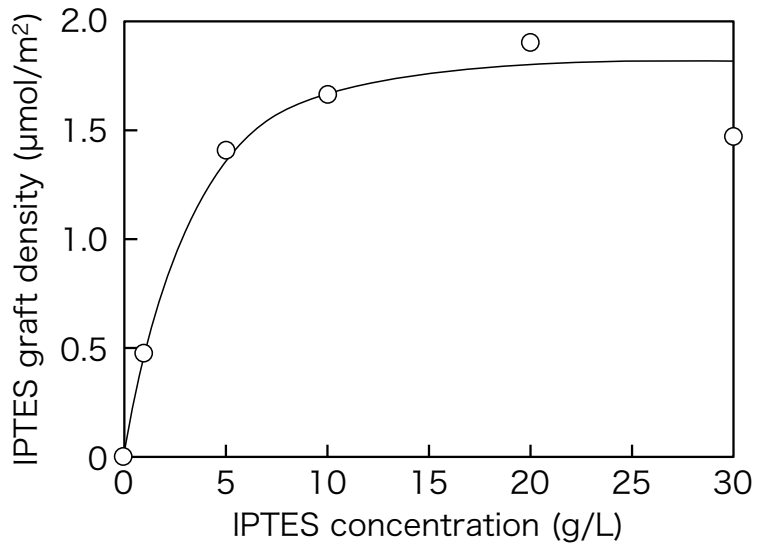


Figure 2

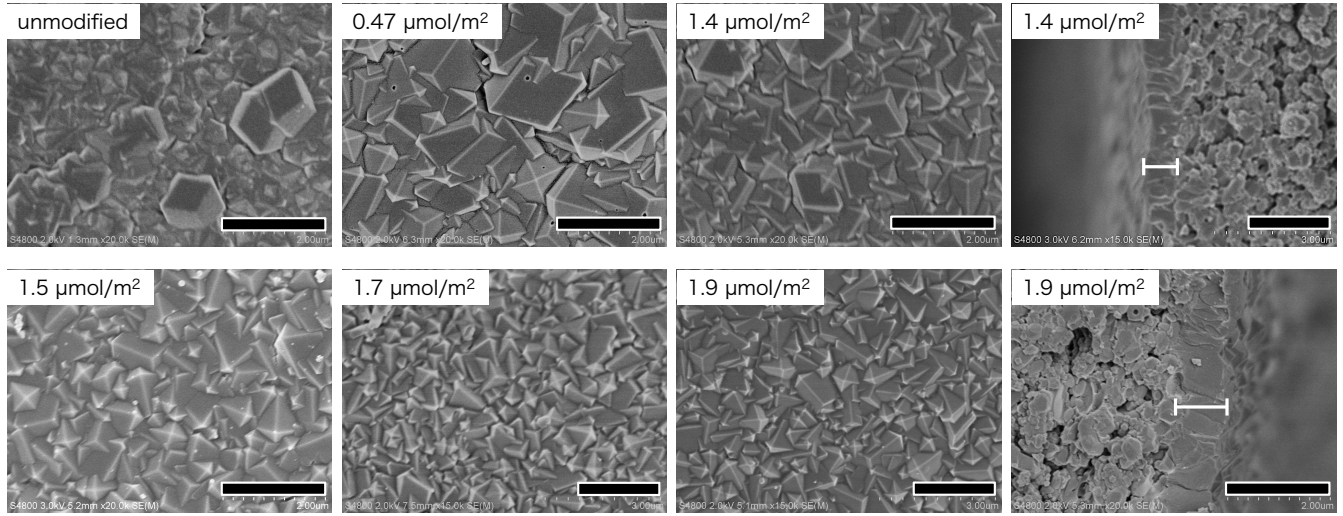


Figure 3

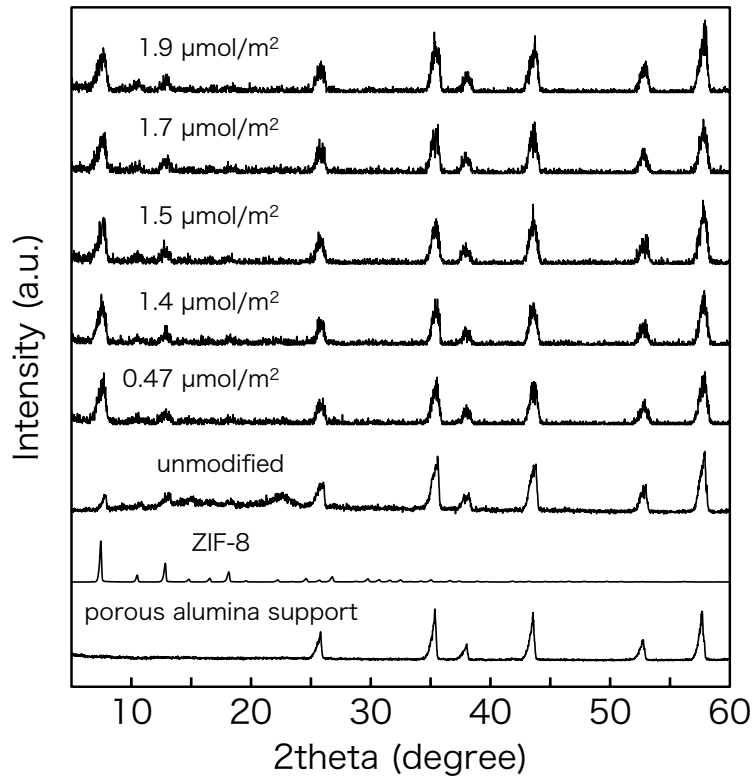


Figure 4

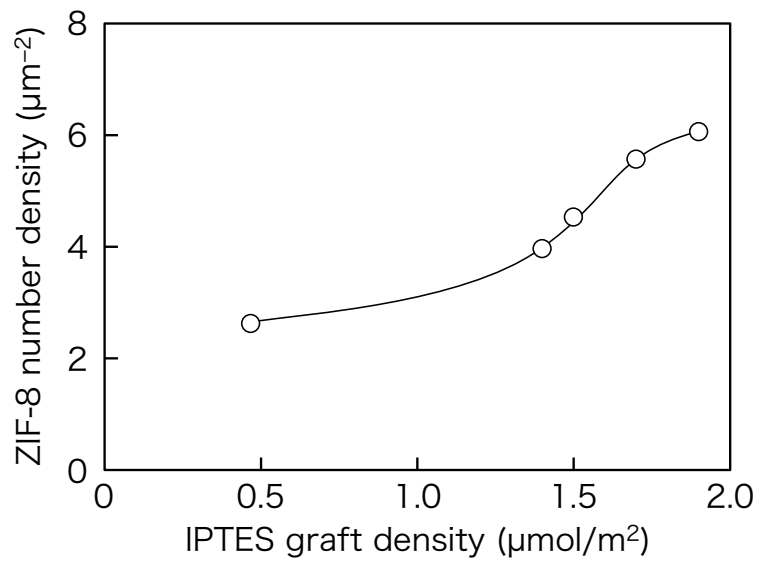


Figure 5

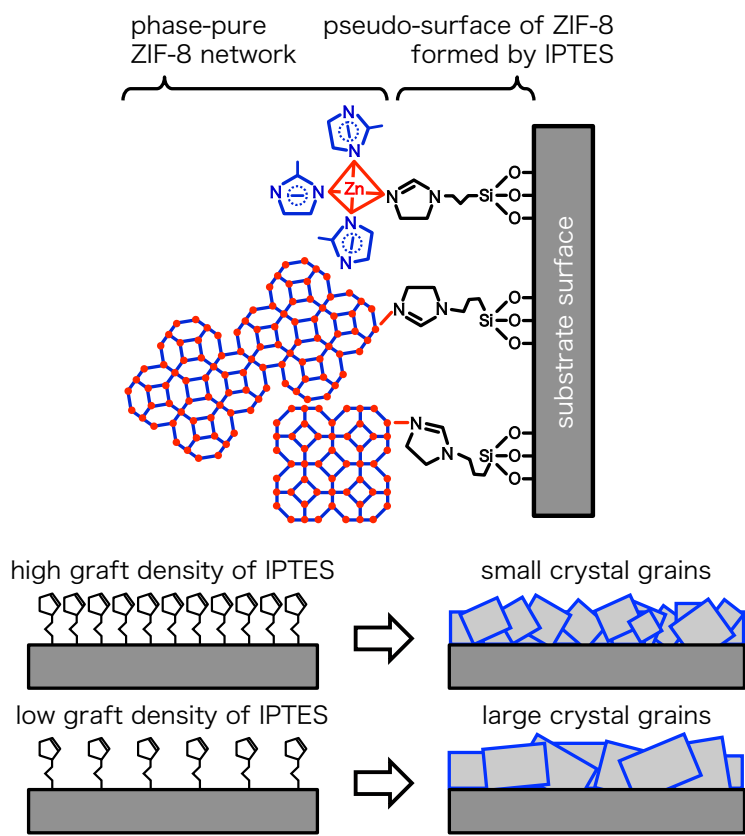


Figure 6

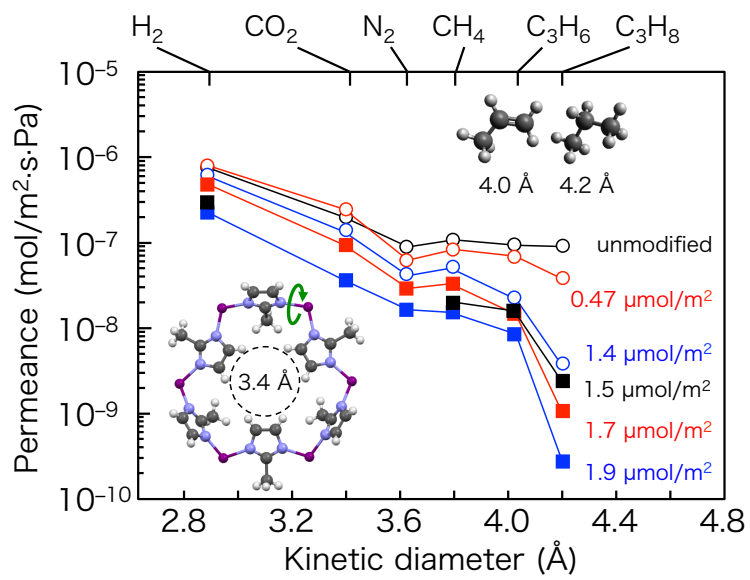


Figure 7

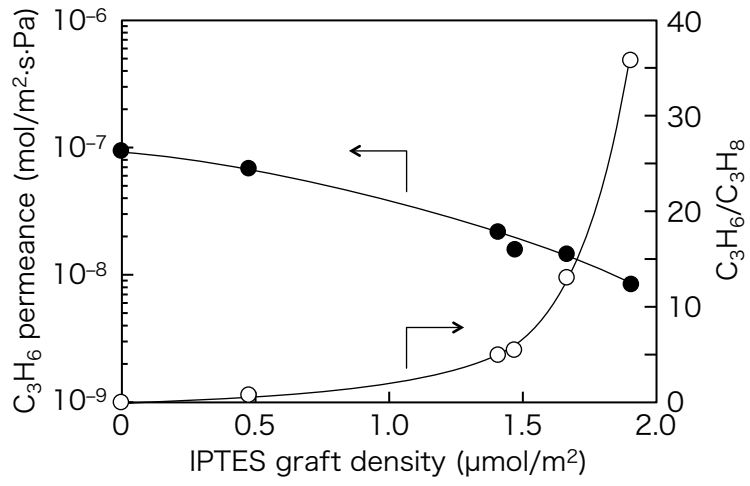


Figure 8

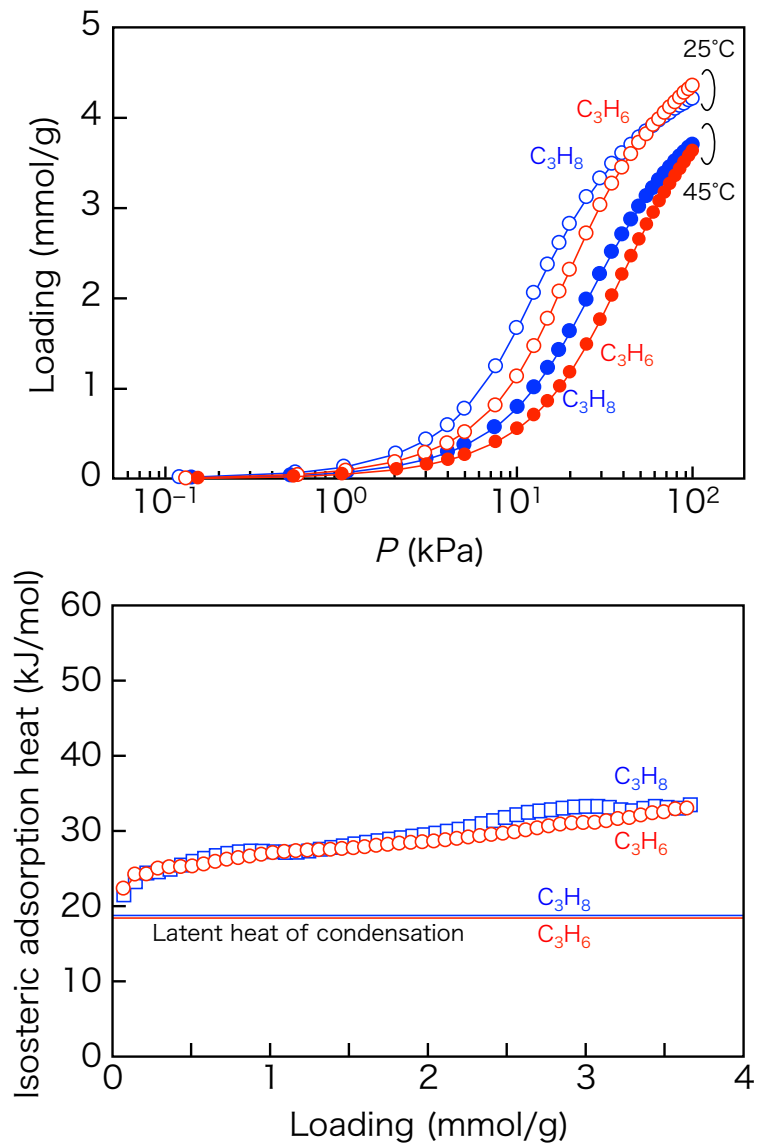


Figure 9

